Observation of strain-relaxation-induced size effects in *p*-type Si/SiGe resonant-tunneling diodes

P. W. Lukey, J. Caro, T. Zijlstra, E. van der Drift, and S. Radelaar
Delft Institute of Microelectronics and Submicron Technology, Faculty of Applied Physics, Delft University of Technology, P.O. Box 5046, NL-2600 GA Delft, The Netherlands

(Received 12 August 1997)

We have studied the effect of strain relaxation in small Si/SiGe resonant-tunneling diodes (RTD's) on the tunneling of holes through these structures. We have used RTD's mesa-etched into dots and wires, the lateral dimensions ranging from 10 μm down to 230 nm. In the dots we find a very strong shift of the light-hole (LH) resonance in the tunneling spectrum as the dot diameter decreases below 1 μm, while the position of the heavy-hole (HH) resonance is constant. In the wires, on the contrary, this size effect in the tunneling is completely absent: both peak positions are constant. This behavior, including the surprising insensitivity of the tunneling spectrum to the wire width, arises from a substantial degree of strain relaxation in the SiGe layers of the devices. This interpretation is supported by the strain dependencies we derive for the HH and LH barrier heights, and the HH-LH splitting in the quantum well. The combined effect of these quantities on the peak voltages agrees qualitatively with the experimental data, when we assume that in the dots the relaxation is biaxial, while in the wires it is predominantly uniaxial. The interpretation is also consistent with magnetotunneling-spectroscopy data, which reflect the in-plane anisotropy of the LH quantum-well subband. We find for all dot diameters a fourfold rotational symmetry of the shift of the LH resonance and for the wires a remarkable transition from a fourfold to a pronounced twofold rotational symmetry of this shift as the wire width decreases below 900 nm. This transition is interpreted as evidence for the strong influence of uniaxial relaxation on the in-plane dispersion. [S0163-1829(98)00604-3]

I. INTRODUCTION

Strain strongly influences the valence band of Si and SiGe. It lifts the degeneracy of the heavy-hole (HH) and light-hole (LH) band edges and determines the dispersion of the HH and LH bands. In *p*-type Si/SiGe devices the SiGe layers are usually coherently strained with respect to the Si substrate. However, it is well established that elastic strain relaxation can occur at Si/SiGe mesa side walls.[1] In structures with small lateral dimensions this leads to a large reduction of the average strain in the SiGe layers, and thus to a dramatic change of their electrical properties. Therefore, size effects in the electrical transport induced by strain relaxation are of great importance in small microelectronic Si/SiGe devices.

Small double-barrier resonant-tunneling diodes (RTD's; see Fig. 1), which are receiving renewed attention in view of application in ultralow power memories,[2] are very well suited to study the effect of strain relaxation on the valence band. For example, the voltage splitting between the first heavy-hole and light-hole resonances (HH_0 and LH_0, respectively) in the *I-V* characteristics of cylindrical Si/SiGe RTD's was recently found to decrease clearly as the mesa diameter falls below 1 μm.[3] This was explained by a reduction of the bulk HH-LH band-edge splitting caused by partial relaxation of the strain in the SiGe layers. Also the in-plane dispersion $E(k_\parallel)$ of the quantum-well subbands can be mapped in RTD's, using magnetotunneling spectroscopy with the magnetic field B in the plane of the quantum well.[4] Holes tunneling to the quantum well over a distance Δz acquire extra kinetic crystal momentum $\hbar\Delta k_\parallel = eB\Delta z$ in the in-plane direction perpendicular to the magnetic field. The resulting peak shift ΔV_p is approximately proportional to $E(\Delta k_\parallel)$. With angle-resolved magnetotunneling spectroscopy, where the peak shifts are measured at different directions of the magnetic field, the in-plane anisotropy of the quantum-well subbands in large-area Si/SiGe,[5,6] InGaAs/AlAs,[7] and GaAs/AlAs (Ref. 8) RTD's was observed.

In this paper, we report a study of the size dependence of resonant tunneling in high-quality Si/SiGe double-barrier dots and wires with lateral dimensions between 230 nm and 10 μm. Surprisingly, while dots show a strong diameter dependence of the HH_0-LH_0 voltage splitting, we find no significant change of the peak voltages in wires of comparable widths. We have studied this interesting effect in more detail using angle-resolved magnetotunneling spectroscopy to

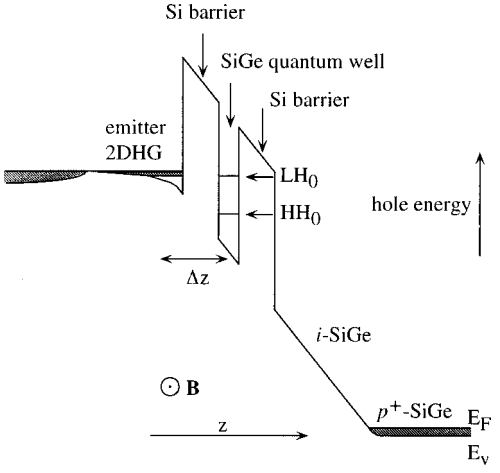

FIG. 1. Schematic overview of the potential profile of a Si/SiGe RTD under applied voltage.

study the strain-relaxation-induced size dependence of the in-plane anisotropy. The result is a fourfold rotational symmetry of the voltage shift of the LH_0 resonance in the dots. In the wires, on the contrary, this symmetry gradually changes to a pronounced twofold rotational symmetry in the narrowest wires.

We attribute the above findings to strain relaxation in the SiGe layers of the devices. This explanation is supported by the strain dependencies we derive for the HH and LH band properties that are relevant to the peak voltages, both for the dots and the wires. For the dots we assume biaxial strain relaxation and for the wires uniaxial strain relaxation. For the wires we also derive the in-plane anisotropy of the LH band. The result of this supports the interpretation that the wire-width dependence of the symmetry of the LH_0 voltage shift is caused by uniaxial strain relaxation.

This paper is organized as follows. The details of the layered Si/SiGe structure and the device fabrication are described in Sec. II. In Sec. III we present the experimental results. First the size dependence of the I-V characteristics of dots and wires is given, then the magnetotunneling-spectroscopy data are presented. In Sec. IV the data are interpreted. The effects of biaxial and uniaxial strain relaxation on the subband-edge energies are analyzed and it is discussed how uniaxial strain relaxation influences the in-plane symmetry of the LH_0 subband. Finally, in Sec. V a summary and the conclusions are given.

II. LAYERED STRUCTURE AND DEVICE FABRICATION

Our devices were fabricated from a layered structure that was grown with solid-source molecular-beam epitaxy on a p^+-type Si (001) wafer. The layer thicknesses were determined with transmission electron microscopy (TEM). The nominally undoped double-barrier region consists of a strained 3.3-nm $Si_{0.78}Ge_{0.22}$ quantum well and two 5.9-nm Si barriers. The 32-nm-thick electrodes adjacent to the barriers are also $Si_{0.78}Ge_{0.22}$. The inner half of the electrodes was nominally undoped to suppress dopant incorporation in the barriers. The layered structure was grown on a 500-nm-thick p^+-type Si buffer and contacted with a 315-nm-thick p^+-type Si cap layer. The B concentration in the p^+ layers is 1×10^{19} cm^{-3}. TEM revealed that dislocations are present at the interfaces between the electrodes and the buffer layer or cap layer. From the dislocation density it was estimated that on the average 8% of the compressive strain in the SiGe layers is relaxed. Further processing was similar to that of Ref. 3. First mesas were etched by reactive-ion etching in a $SiCl_4/Cl_2$ plasma using a chromium mask fabricated by electron-beam lithography and lift-off. After removal of the mask SiO_2 was deposited at $T=350$ °C by plasma-enhanced chemical vapor deposition. The mesa top was uncovered by chemical mechanical polishing followed by etch-back of the SiO_2 layer. Al-Si(1%) and Al were used for metallization on the top and the backside, respectively. Finally, the chips were annealed in forming gas at $T=400$ °C to improve the contact quality. Dots with diameters d between 230 nm and 10 μm and 1.1-μm-long wires with widths w between 250 and 900 nm were fabricated on the same chip. The wires were oriented along a $\langle 110\rangle$ axis to within 1°. The ratio between the total thickness of the SiGe layers and the dot diameter or wire width is such ($\sim$1:3.5 in the smallest devices) that strong elastic strain relaxation can be expected. This follows from the amount of strain relaxation in SiGe wires fabricated on Si substrates. It was shown by Raman measurements and finite element calculations that the amount of strain relaxation in the middle of the surface layer of such a wire is larger than 20% if the ratio between height and width of the wire is larger than 1:20.[9,10]

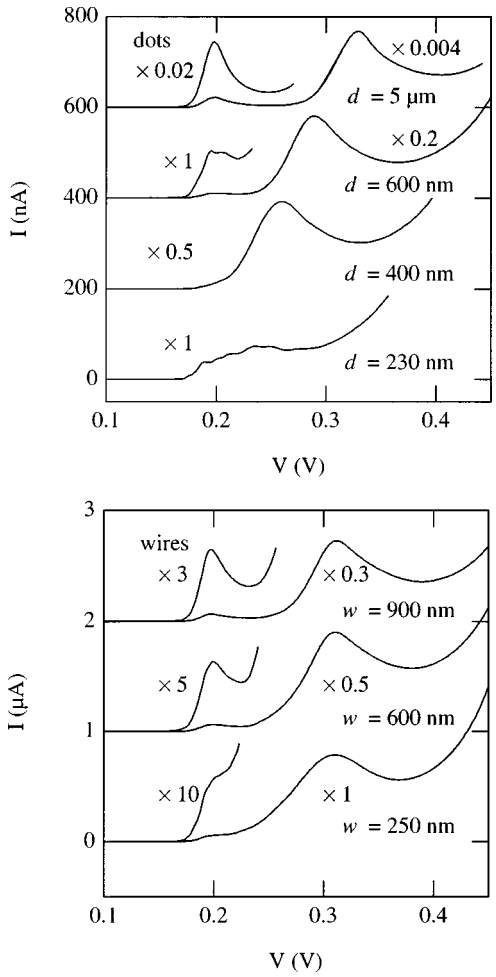

FIG. 2. I-V characteristics of dots with diameters d and wires with widths w ($T=4.2$ K). The voltage is applied to the top electrode. The characteristics of the larger devices have been offset for clarity and multiplication factors of the current are indicated.

III. EXPERIMENTAL RESULTS

A. I-V characteristics

Two-point I-V measurements were performed at $T=4.2$ K. The I-V characteristics were nearly identical for positive and negative bias voltage. Typical examples are shown in Fig. 2 for dots and for wires. In the $d=10$ μm dots (of which the curves are not shown) and the 5 μm dots two resonances with negative differential resistance are observed for both current directions. In the emitter only HH states are occupied due to the strain-induced HH-LH splitting, so that tunneling particles initially are heavy holes. The first resonance at $|V_p|\approx200$ mV is due to resonant tunneling via the HH_0 quantum-well subband and the second corresponds to

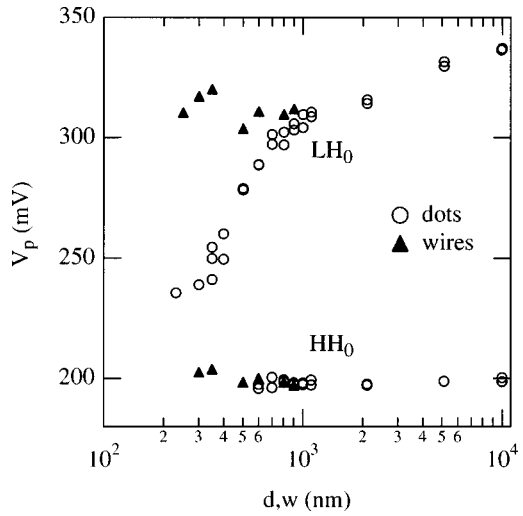

FIG. 3. Peak voltage measured at positive bias voltage vs lateral dimension, for dots and wires ($T=4.2$ K).

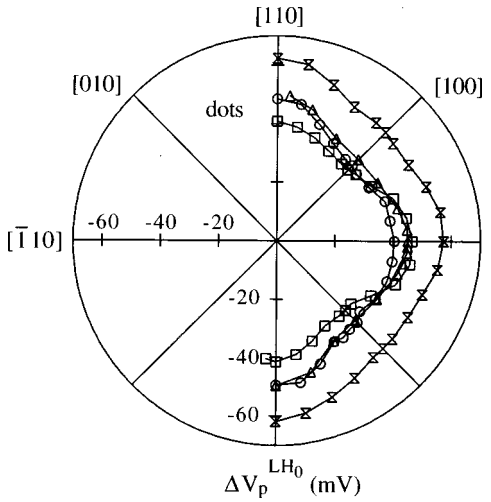

FIG. 4. Polar plot of the voltage shift of the LH_0 resonance at $B=14$ T with respect to the $B=0$ T resonance voltage vs the direction of $\Delta k_\parallel$. The shifts were measured at positive bias voltage in (○) 230-nm, (□) 400-nm, (△) 1100-nm, and (⧖) 5-μm dots ($T=1.7$ K). The lines are guides to the eye.

the LH_0 quantum-well subband. The peak-to-valley ratios of the HH_0 and LH_0 resonances are 1:4.6 and 1:2.2, respectively. This is comparable to the highest values reported for Si/SiGe RTD's.[11,12]

In Fig. 2 it is seen that the LH_0 resonance undergoes a strong shift to lower voltage with decreasing dot diameter, while the position of the HH_0 resonance is constant. For the wires the situation is different, since in these, both resonances stay at the same voltage for decreasing width. The observed behavior is shown more clearly in Fig. 3, where the peak voltages $V_p^{HH_0}$ and $V_p^{LH_0}$ are plotted as a function of dot diameter and wire width. For the dots $V_p^{LH_0}$ drops from 337 mV in the 10-μm dot to 236 mV in the 230-nm dot. The data points for the HH_0 peak are limited to the dots with $d \geqslant 600$ nm. The reason is that for $d<600$ nm the determination of $V_p^{HH_0}$ is not reliable because of the absence of negative differential resistance, which is partially due to overlap of the two resonances. The ratio $I_p^{HH_0}/I_p^{LH_0}$ of the HH_0 and LH_0 peak currents decreases with decreasing dot diameter. For the wires this effect is absent. Finally, we note that for the smaller dots the HH_0 resonance and to a lesser extent the LH_0 resonance have fine structure. In Fig. 2 this can be seen in the I-V characteristics of the 600- and 230-nm dots. Also the narrower wires show weak fine structure in the resonances. The geometrical size of the devices is too large to lead to quantum confinement in the lateral direction. Still, side-wall depletion and inhomogeneous strain relaxation may well lead to smaller electrical dimensions, and therefore, the fine structure in the smallest devices may arise from lateral confinement. In addition, inhomogeneous elastic strain relaxation can lead to lateral quantum confinement in a ring near the side wall of the dot.[13] This mechanism could be responsible for the fine structure in larger devices, such as the 600-nm dot. However, also tunneling through defect states can give rise to fine structure, as has been observed in $GaAs/Al_xGa_{1-x}As$ RTD's.[14]

Possible explanations for the strong shift of $V_p^{LH_0}$ in the dots are (i) series resistance effects, (ii) quantum confinement in the lateral directions, and (iii) strain relaxation. Series resistance could cause the observed shift, if the voltage drop across the series resistance is larger in large-area devices than in small dots. However, this would also cause a shift of the HH_0 resonance, which is not observed. In addition, an upper boundary for the voltage drop across the series resistance is given by the differential resistance measured beyond the LH_0 valley (assuming that the series resistance is Ohmic). This upper boundary is much smaller than the observed LH_0 shift. Thus, series resistance effects do not explain the results. Quantum confinement of carriers in the well would give rise to splitting of the two-dimensional (2D) LH_0 subband into 0D states, which lie above the bottom of the original subband. In the emitter lateral confinement is weaker, due to stronger screening. Therefore, one expects a peak shift towards higher voltages as the dot diameter becomes smaller, in contrast to the observed shift towards lower voltage. Thus, also quantum confinement can be ruled out. This leaves strain relaxation as the explanation for the observed shift of $V_p^{LH_0}$, which agrees with Ref. 3. Since the wire widths and the dot diameters are in the same range, it seems contradictory that no peak shifts are observed for the wires. In Sec. IV we will discuss this in detail.

B. Magnetotunneling spectroscopy of the LH_0 resonance

In the dots and wires we also performed angle-resolved magnetotunneling-spectroscopy measurements, at $T=1.7$ K and $B=14$ T. At this magnetic field the magnetic length is $l_m=(\hbar/eB)^{1/2}=6.9$ nm, which exceeds the quantum-well width. Hence, the diamagnetic shift of the quantum-well subbands should be negligible.[15] The samples were rotated *in situ*. Reference measurements at $B=0$ T were performed at the same temperature. Results for the LH_0 resonance are presented here, because in the smaller devices the HH_0 resonance could not be identified unambiguously for each field direction, neither in the I-V nor in the dI/dV-V characteristics.

Figure 4 shows the peak shift $\Delta V_p^{LH_0}=V_p^{LH_0}(14\text{ T})-V_p^{LH_0}(0\text{ T})$ for different directions of $\Delta k_\parallel$ for four dots of

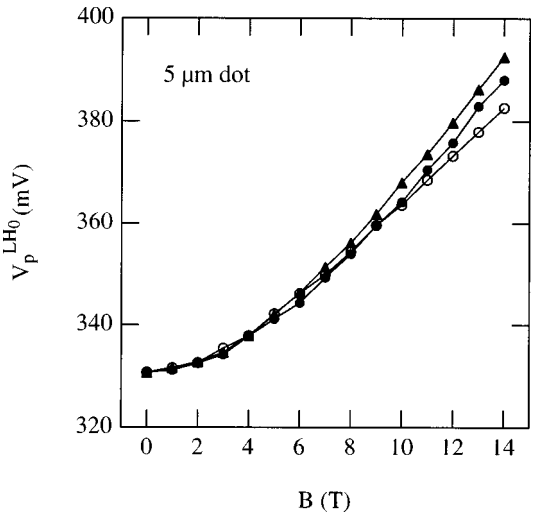

FIG. 5. $V_p^{LH_0}$ as a function of B, measured for different directions of $\Delta k_\parallel$ in a 5-μm dot ($T=1.7$ K); (●) $\Delta k_\parallel \| [1\bar{1}0]$, (○) $\Delta k_\parallel \| [010]$, (▲) $\Delta k_\parallel \| [1\ \bar{1}0]$. The anisotropy of the peak shift becomes more pronounced for $B \geq 8$ T.

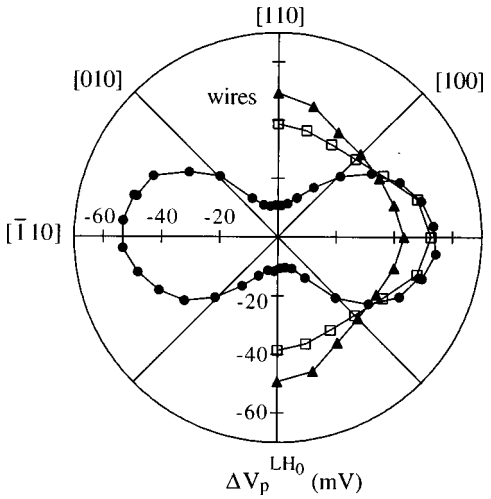

FIG. 6. Polar plot of the peak voltage shift of the LH_0 resonance at $B=14$ T with respect to the $B=0$ T resonance voltage vs the direction of $\Delta k_\parallel$. The shifts were measured at positive bias voltage in (●) 250-nm, (□) 600-nm, and (▲) 900-nm wires ($T=1.7$ K). In the 900-nm wire the polar plot has approximately a fourfold rotational symmetry. As the wires become narrower, the symmetry is reduced to twofold rotational symmetry with the same mirror axes as those of the wires. The lines are guides to the eye.

different diameter. The polar plots for the three smaller dots are closely grouped together at a distinct distance from the curve of the 5-μm dot. All curves deviate from a circular shape and are approximately fourfold rotational symmetric when folded, reflecting the warping of the LH_0 subband and the symmetry of the SiGe (001) lattice plane. In all dots the maximum peak shift is measured for $\Delta k_\parallel \| \langle 110 \rangle$. The amount of warping for a 5-μm dot is made more clear in Fig. 5, which shows $V_p^{LH_0}$ versus B for three directions of $\Delta k_\parallel$. The anisotropy starts to be appreciable above ~ 8 T. Also it is seen that the curves do not show perfectly the expected symmetry, since the peak shifts measured for $\Delta k_\parallel \| [110]$ and for $\Delta k_\parallel \| [\bar{1}10]$ differ.

Figure 6 shows examples of polar plots of $V_p^{LH_0}$ for three wires. Clearly, these plots develop in a completely different way with decreasing lateral size. The plot for the 900-nm wire is again approximately fourfold rotational symmetric. For smaller wires it is twofold rotational symmetric and with decreasing wire width it is increasingly squeezed in the $\langle 110 \rangle$ direction parallel to the wire. For the 250-nm wire the result is a strongly altered polar plot, in which the peak shift is five times as large for $\Delta k_\parallel \perp$ wire than for $\Delta k_\parallel \|$ wire. This strong anisotropy is present over a wide magnetic-field range, as is illustrated in Fig. 7.

We have also determined the angular dependence of the LH_0 peak current $I_p^{LH_0}$, for the dots and for the wires. The results are plotted in Fig. 8 for a 5-μm dot, and for 600- and 250-nm wires. In each dot and in the 900-nm wire $I_p^{LH_0}$ is largest for $\Delta k_\parallel \| \langle 100 \rangle$. In the wires the anisotropy changes gradually. Eventually, in 250–350-nm-wide wires $I_p^{LH_0}$ has a completely different behavior, since it is maximum for $\Delta k_\parallel \| \langle 100 \rangle$.

IV. INTERPRETATION

Our main experimental results are a decrease of the HH_0-LH_0 peak splitting with decreasing dot diameter, a constant HH_0-LH_0 peak splitting with decreasing wire width, and a transition from fourfold to twofold rotational symmetry of the polar plot of the LH_0 peak-voltage shift, when changing from dots to narrow wires. To interpret these results we follow Zaslavsky *et al.*,[3] who explained a reduction of the HH_0-LH_0 peak splitting in dots of similar size with strain relaxation in the SiGe layers. We argue that the different results on dots and wires can be explained by assuming that the relaxation is biaxial in the dots and uniaxial in the wires. For both sets of devices we explain the observed behavior of the HH_0 and LH_0 peak voltages qualitatively by analyzing the effect of relaxation on the barrier heights and the HH-LH band-edge splitting. Finally, we determine the influence of uniaxial relaxation on the in-plane dispersion of

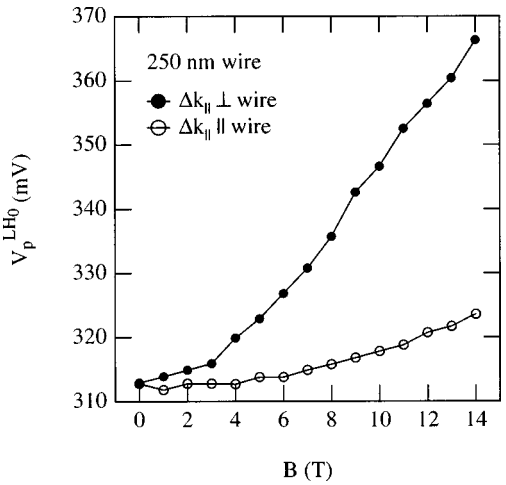

FIG. 7. $V_p^{LH_0}$ as a function of B, measured for different directions of $\Delta k_\parallel$ in a 250-nm wire ($T=1.7$ K). The anisotropy between the directions perpendicular and parallel to the wire is present over the full magnetic-field range.

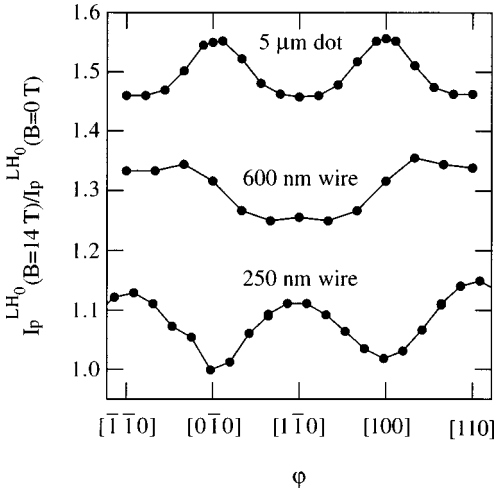

FIG. 8. Peak current of the LH_0 resonance $I_p^{LH_0}$ at $B=14$ T, normalized to the peak current at $B=0$ T, vs the direction φ of $\Delta k_\parallel$ ($B=14$ T; $T=1.7$ K). In large wires and in all dots the peak current is maximum for $\Delta k_\parallel \parallel \langle 100\rangle$. For decreasing wire width this gradually changes and in the $w=250$ nm wires the current peaks for $\Delta k_\parallel \parallel \langle 110\rangle$. The curves of the 600-nm wire and the 5-μm dot have an offset of 0.2 and 0.4, respectively.

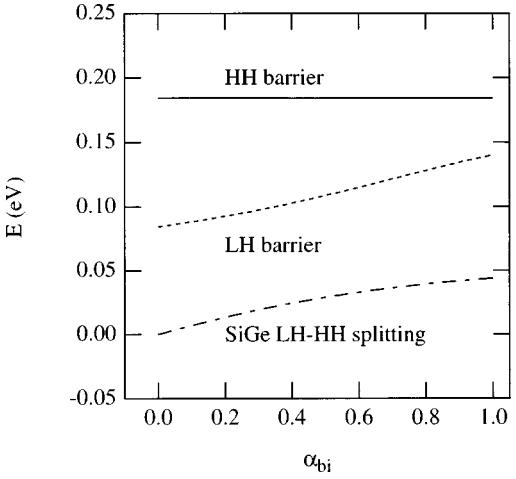

FIG. 9. Heavy-hole and light-hole barrier heights and SiGe HH-LH band-edge splitting as a function of the reduced in-plane biaxial strain $\alpha_{bi}=\varepsilon_\parallel^{SiGe}/\varepsilon_{\parallel,coh}^{SiGe}$ in the quantum well. The HH and LH barriers are measured with respect to the HH and LH band edges in the SiGe, respectively.

the LH band to show that this can cause the size dependence of the magnetotunneling-spectroscopy data.

A. Effect of biaxial strain relaxation on the *I-V* characteristics

In the dots the strain is expected to be nonuniform both in the lateral and in the vertical direction. For simplicity we use a uniform, but material-dependent strain, which is assumed to be biaxial. We first briefly summarize some properties of the valence band, valid in biaxially strained SiGe grown on a (001) Si substrate. For $\Delta k_\parallel=0$ the HH band does not mix with the LH band and the spin-orbit split-off (SO) band, irrespective of the amount of strain relaxation in the dot. Further, the HH effective mass in the current direction is independent of strain, both in the barriers and the well. Consequently, the HH barrier height is the only strain-dependent parameter that determines the energy of the HH_0 subband edge in the well. For the LH_0 subband edge the situation is different. Strain relaxation reduces the HH-LH band-edge splitting in the well. Further, strain relaxation in the SiGe layers is accompanied by a buildup of tensile strain in the Si barriers. This splits the HH and LH bands in the Si, resulting in a lowering of the LH barrier with respect to the HH barrier. This is contrary to the situation in the compressively strained SiGe layers, where the HH band forms the valence-band edge.

First, we consider the HH_0 resonance. To understand the independence of $V_p^{HH_0}$ on dot diameter and therefore on the amount of strain relaxation, we use the results of Ref. 16. The strain dependence of the band offset, i.e., of the barrier height, can be calculated from the strain-induced shift of the bulk band edges. Rewriting results from Ref. 16, we arrive at $E_{HH}(\varepsilon_\parallel)$, the strain-dependent energy of the heavy-hole band edge of Si or SiGe:

$$E_{HH}(\varepsilon_\parallel)=E_0+\frac{\Delta_0}{3}+2a_\nu\varepsilon_\parallel\left(1-\frac{c_{12}}{c_{11}}\right)+b\varepsilon_\parallel\left(1+2\frac{c_{12}}{c_{11}}\right). \tag{1}$$

Here E_0 is the material-dependent average energy of the HH, LH, and SO band edges with respect to a fixed reference point in the absence of strain, $\varepsilon_\parallel$ is the in-plane strain, Δ_0 is the spin-orbit splitting, a_ν and b are deformation potentials, and c_{11} and c_{12} are elastic constants. The strain-dependent barrier height $E_{b,HH}$ is now given by the difference between the SiGe and Si terms as determined by Eq. (1):

$$E_{b,HH}(\varepsilon_\parallel^{SiGe})=E_{HH}^{SiGe}(\varepsilon_\parallel^{SiGe})-E_{HH}^{Si}[\varepsilon_\parallel^{Si}(\varepsilon_\parallel^{SiGe})]. \tag{2}$$

$\varepsilon_\parallel^{Si}$ ($\varepsilon_\parallel^{SiGe}$) can be evaluated by assuming that the in-plane lattice constants in the barriers and the quantum well are equal. This means that the in-plane strains in the Si and SiGe are related via the bulk Si and SiGe lattice constants a_0^{Si} and a_0^{SiGe}:

$$\varepsilon_\parallel^{Si}(\varepsilon_\parallel^{SiGe})=(1+\varepsilon_\parallel^{SiGe})\,\frac{a_0^{SiGe}}{a_0^{Si}}-1. \tag{3}$$

We have evaluated Eq. (2) for $x=0.22$, the Ge fraction in our devices. For $Si_{0.78}Ge_{0.22}$ deformation potentials, elastic constants, and the bulk lattice constant were obtained by linear interpolation between the Si and Ge values, taken from Ref. 17. The strain-independent term of Eq. (1) was fixed using the relation $E_{b,HH}(\varepsilon_{\parallel,coh}^{SiGe})=0.84x$ eV for coherently strained $Si_{1-x}Ge_x$ grown on Si.[18] The final result is shown in Fig. 9. Clearly, the heavy-hole barrier height is virtually independent of the strain. This implies that the HH_0 subband-edge energy is independent of the strain state of the double-barrier structure, in agreement with our observation that $V_p^{HH_0}$ is independent of the diameter of the dots.

To explain the size dependence of $V_p^{LH_0}$, we now analyze the LH barrier height measured with respect to LH band edge in the SiGe. It can be derived by correcting the HH barrier

height for the strain-induced band-edge splittings in the Si and SiGe. These splittings also follow from Ref. 16:

$$E_{\mathrm{LH}}-E_{\mathrm{HH}}=-\tfrac{1}{2}(\Delta_0-\kappa)+\tfrac{1}{6}\sqrt{(3\Delta_0+\kappa)^2+8\kappa^2}, \quad (4a)$$

with

$$\kappa=-3b\left(1+2\frac{c_{12}}{c_{11}}\right)\varepsilon_{\parallel}. \quad (4b)$$

The resulting strain dependence of the LH barrier is plotted in Fig. 9. In this figure we also show the strain dependence of $E_{\mathrm{HH}}^{\mathrm{SiGe}}-E_{\mathrm{LH}}^{\mathrm{SiGe}}$, the HH-LH band-edge splitting in the SiGe well. The value of the SiGe spin-orbit splitting was obtained by linear interpolation of the Si and Ge values. From Fig. 9 it is seen that both the LH barrier height, measured with respect to the LH band edge in the well, and the HH-LH band-edge splitting in the well decrease strongly due to strain relaxation. Both effects are expected to lead to a strong lowering of the LH_0 level in the quantum well. Therefore, the decrease of $V_p^{\mathrm{LH}_0}$ for decreasing dot diameter can be explained by biaxial strain relaxation. To prove this rigorously, the strain dependence of the LH_0 subband should be calculated using the envelope-function approximation including the mixing of the LH and SO bands. Also admixture of the HH band should be included, since coherent tunneling from the HH emitter states to the LH_0 subband only takes place for $k_{\parallel}\neq 0$ (unless the strain is almost completely relaxed, which would lift the HH-LH splitting and lead to population of LH emitter states). Finally, we remark that the lowering of the LH barrier is also expected to contribute to the relatively high LH_0 peak current that was observed in the small dots, since it leads to a higher transmission probability of the barriers.

It is difficult to estimate the average amount of strain relaxation in the smallest dots from $V_p^{\mathrm{LH}_0}$. A rough estimate can be made following Ref. 3, where only the reduction of the HH-LH band-edge splitting in the well was taken into account. This yields a strain relaxation of $\sim 80\%$ in the 230-nm dot (assuming that the peak voltages are proportional to the subband-edge energies). In comparison with the results of Ref. 3 the size dependence of $V_p^{\mathrm{LH}_0}$ is stronger, indicating that more strain is relaxed. This is as expected, since in our devices the SiGe electrodes are thicker and have a constant instead of a graded Ge content.

B. Effect of uniaxial strain relaxation on the *I-V* characteristics

In the wires $V_p^{\mathrm{HH}_0}$ and $V_p^{\mathrm{LH}_0}$ are independent of the width. At first sight, this suggests that the SiGe layers are still coherently strained. However, this seems unlikely in view of the strong relaxation in the dots. Furthermore, the twofold rotational symmetry of the polar plot of $V_p^{\mathrm{LH}_0}$ measured in the 250-nm wire points to symmetry reduction of the in-plane dispersion and is therefore a strong indication of strain relaxation. To solve this apparent contradiction we analyze below the influence of uniaxial strain relaxation on the barrier heights and on the HH-LH band-edge splitting in the well.

The barrier heights are derived from the strain dependence of the band-edge energies, as was also done in the case of biaxial strain relaxation. Since no analytic expressions are available for the band-edge energies, the strain-dependence is now calculated using a Hamiltonian composed of a 6×6 spin-orbit interaction Hamiltonian and a 3×3 strain Hamiltonian.[19,20] The band-edge energies are then given by $E^{\mathrm{HH/LH}}=E_0+\Delta E^{\mathrm{HH/LH}}$, where ΔE^{HH} and ΔE^{LH} are eigenvalues of the Hamiltonian and E_0 is again the average energy of the HH, LH, and SO bands in the absence of strain with respect to a fixed reference point.

In the calculation we replace the nonuniform strain by an average value, as was also done for the dots. The strain tensor is taken from Ref. 11. First it is derived in wire coordinates x', y', and z', parallel to the crystal axes [110], [1$\bar{1}$0], and [001], respectively. The longitudinal and transverse directions of the wire are taken as the x' and y' directions. We assume that the strain component in the longitudinal direction of the wire equals the misfit, which should be a good approximation given the length of the wire. The small amount of strain relaxation due to the presence of misfit dislocations is neglected. The three shear strain components are zero due the symmetry of the wire in the x'-y' plane. The stress in the vertical direction is also taken zero. Thus, of the six independent strain components and six independent stress components, which are related to each other by Hooke's equation, four strain components and one stress component are known. Only one independent element is left, the strain in the transverse direction. This is treated as an adjustable reduced strain parameter α_{uni}, defined as the ratio of the strain in the y' direction and the strain in the $\langle 110\rangle$ direction in a coherently strained film. Solving Hooke's equation now yields the SiGe strain tensor ε' in wire coordinates:

$$\varepsilon_{xx}'^{\mathrm{SiGe}}=\frac{a_0^{\mathrm{Si}}-a_0^{\mathrm{SiGe}}}{a_0^{\mathrm{SiGe}}}, \quad (5a)$$

$$\varepsilon_{yy}'^{\mathrm{SiGe}}=\alpha_{\mathrm{uni}}\varepsilon_{xx}'^{\mathrm{SiGe}}, \quad (5b)$$

$$\varepsilon_{zz}'^{\mathrm{SiGe}}=-\frac{c_{12}}{c_{11}}(1+\alpha_{\mathrm{uni}})\varepsilon_{xx}'^{\mathrm{SiGe}}, \quad (5c)$$

$$\varepsilon_{ij}'^{\mathrm{SiGe}}=0 \quad \text{for } i\neq j, \quad (5d)$$

with $H=2c_{44}+c_{12}-c_{11}$. Here the elastic constants of $\mathrm{Si}_{1-x}\mathrm{Ge}_x$ are used. For $\alpha_{\mathrm{uni}}=1$ the SiGe is coherently strained. For purely uniaxially stressed SiGe the stress component $\sigma_{yy}'=0$. This corresponds to $\alpha_{\mathrm{uni}}=[-c_{11}(c_{12}-H/2)+c_{12}^2]/[c_{11}(c_{11}+H/2)-c_{12}^2]=-0.056$. As expected, the SiGe is under tensile strain in the transverse direction if $\sigma_{yy}'=0$.

Next, the strain tensor in the Si barriers is derived. As for the SiGe it is assumed that $\sigma_{zz}'=0$ and that the shear strain components are again zero due to symmetry. The other strain components are calculated by imposing that the in-plane lattice constants in the barriers and the well are equal and by solving Hooke's equation. The resulting strain tensor is given by

$$\varepsilon_{xx}'^{\mathrm{Si}}=0, \quad (6a)$$

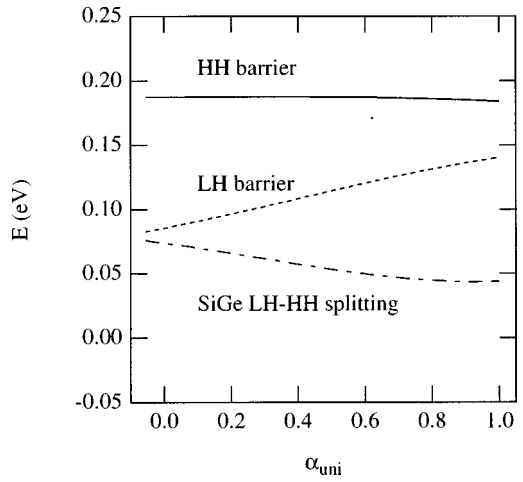

FIG. 10. Heavy-hole and light-hole barrier heights and SiGe HH-LH band-edge splitting as a function of the reduced uniaxial strain α_{uni} in the transverse in-plane direction. The HH and LH barriers are measured with respect to the HH and LH band edges in the SiGe, respectively.

$$\varepsilon'^{\text{Si}}_{yy} = -1 + (1 + \varepsilon'^{\text{SiGe}}_{yy}) \frac{a_0^{\text{SiGe}}}{a_0^{\text{Si}}}, \tag{6b}$$

$$\varepsilon'^{\text{Si}}_{zz} = -\frac{c_{12}}{c_{11}} \varepsilon'^{\text{Si}}_{yy}, \tag{6c}$$

$$\varepsilon'^{\text{Si}}_{ij} = 0 \quad \text{for } i \neq j, \tag{6d}$$

where the Si elastic constants are used.

Finally, the Si and SiGe strain tensors are transformed to crystal coordinates. This yields

$$\varepsilon = \begin{pmatrix} \frac{1}{2}(\varepsilon'_{xx} + \varepsilon'_{yy}) & \frac{1}{2}(\varepsilon'_{xx} - \varepsilon'_{yy}) & 0 \\ \frac{1}{2}(\varepsilon'_{xx} - \varepsilon'_{yy}) & \frac{1}{2}(\varepsilon'_{xx} + \varepsilon'_{yy}) & 0 \\ 0 & 0 & \varepsilon'_{zz} \end{pmatrix}. \tag{7}$$

The nonzero off-diagonal strain elements give rise to mixing of the HH band with the LH and SO bands.

With Eqs. (5)–(7) for the strain the eigenvalues of the Hamiltonian were computed for different values of α_{uni}. The final results of the calculation, the HH and LH barrier heights and the HH-LH band-edge splitting in the SiGe, are depicted in Fig. 10. The HH barrier is only slightly higher for uniaxially stressed SiGe than for coherently strained SiGe. If we assume that despite the band mixing the holes tunneling to the HH_0 subband mainly see the HH barrier, it becomes clear that the HH_0 resonance voltage is virtually independent of the wire width. The LH barrier, measured with respect to the LH band edge in the SiGe, is lowered due to relaxation. The HH-LH splitting, on the other hand, increases due to uniaxial strain relaxation, after a small decrease for $0.9 < \alpha_{\text{uni}} \leqslant 1$. Thus the strain dependencies of the LH barrier height and the HH-LH splitting in the well have opposite effects on the LH subband energy for $\alpha_{\text{uni}} < 0.9$ and it is not clear from this analysis whether it increases or decreases due to relaxation. Hence, it is understandable that the LH_0 resonance does not shift significantly as the wire becomes narrower. Finally, it is remarkable that the lowering of the LH barrier does not result in an increase of the LH_0 peak current with respect to the HH_0 peak current for decreasing size, as was observed in the dots. Possibly, this can be explained by a calculation of the current incorporating the band mixing in the correct way.[21]

C. Effect of uniaxial relaxation on the in-plane anisotropy of the LH_0 subband

The angular dependence of the peak shift measured with magnetotunneling spectroscopy is usually interpreted as a direct representation of the in-plane anisotropy of a subband. We assume that this is also valid in our submicrometer devices, keeping in mind that the anisotropy is expected to depend on the position in the wire because of the nonuniform strain. Hence, it seems highly probable that the twofold rotational symmetry observed in the small wires (Fig. 6) is a consequence of uniaxial strain relaxation. The measurements on the dots provide evidence that biaxial strain relaxation has only little influence on the in-plane dispersion of the LH_0 subband.

To check whether uniaxial strain relaxation indeed influences the anisotropy strongly, the in-plane dispersion in partly relaxed SiGe is derived below. This was done by calculation of the eigenvalues of the same Hamiltonian as used in the previous section with a $\mathbf{k}\cdot\mathbf{p}$ Hamiltonian[22] added. The $Si_{1-x}Ge_x$ band parameters used were obtained by linear interpolation between the Si and Ge values of Ref. 17. We assumed that half of the stress in the transverse direction was relaxed, corresponding to $\alpha_{\text{uni}} = 0.472$. For our purpose it is sufficient to calculate the anisotropy of the bands in ''bulk'' $Si_{0.78}Ge_{0.22}$, without using the envelope-function approximation for our heterostructure. Still, we have taken quantum confinement tentatively into account in the following way. The LH_0 subband-edge energy E^{LH_0} can be roughly estimated from the measured $V_p^{\text{LH}_0}$ by assuming that the ratio $E^{\text{LH}_0}/V_p^{\text{LH}_0}$ is determined by the thicknesses of the undoped layers[23] and equals

$$E^{\text{LH}_0}/V_p^{\text{LH}_0} = (b + \tfrac{1}{2}w)/(2b + w + s) = 0.243, \tag{8}$$

where b, w, and s are the thicknesses of the barriers, the quantum well, and the collector spacer layer, respectively. This yields $E^{\text{LH}_0} = 75$ meV for the 250-nm wire. The wave vector k_z for which the bulk SiGe LH energy $E^{\text{LH}}(k_z, k_\parallel = 0)$ is also 75 meV is $k_z = 3.1 \times 10^8\ \text{m}^{-1}$, which is used in the calculations. Finally, we set the in-plane wave vector $\Delta k_\parallel = eB\Delta z/\hbar = 2.8 \times 10^8\ \text{m}^{-1}$, where we used $B = 14$ T and a value for the tunneling distance of $\Delta z = \frac{1}{2}w + b + \lambda \cong 13$ nm. The average distance λ of the emitter holes to the barrier was estimated using the Fang-Howard model.[24] This model assumes that the holes are 2D, as was the case in large area RTD's fabricated from an almost identical layered structure.

The calculation yields $\Delta E^{\text{LH}}(\Delta k_\parallel) = E^{\text{LH}}(k_z, \Delta k_\parallel) - E^{\text{LH}}(k_z, k_\parallel = 0)$ for different angles of $\Delta k_\parallel$. The resulting polar plot is shown in Fig. 11. To compare this with the measurements on the 250-nm wire the peak shifts were transformed to values of $E^{\text{LH}_0}(\Delta k_\parallel) - E^{\text{LH}_0}(k_\parallel = 0)$ using Eq. (8). Clearly, the calculated curve adopts the twofold symmetry of the partially relaxed lattice and $\Delta E^{\text{LH}}(\Delta k_\parallel)$ is considerably larger for $\Delta k_\parallel \perp$ wire than for $\Delta k_\parallel \parallel$ wire. This qualitative

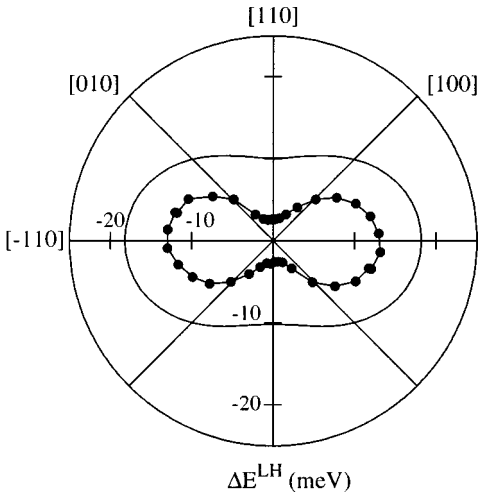

FIG. 11. Polar plot of the calculated values of $\Delta E^{\mathrm{LH}}(\Delta k_{\|})$ vs the direction of $\Delta k_{\|}$ for $\alpha_{\mathrm{uni}}=0.472$, $k_z=3.1\times10^8\ \mathrm{m}^{-1}$, and $\Delta k_{\|}=2.8\times10^8\ \mathrm{m}^{-1}$ (–). The plot also shows $E^{\mathrm{LH}_0}(\Delta k_{\|})-E^{\mathrm{LH}_0}(k_{\|}=0)$ as derived from the peak shifts measured in the 250-nm wire at $B=14$ T (●).

agreement of the model calculations with the measurements supports the interpretation that the in-plane anisotropy of the peak shift is due to uniaxial strain relaxation. The quantitative difference is not surprising in view of the simplicity of the model. Furthermore, the outcome of the model is sensitive to the estimated values of k_z and $\Delta k_{\|}$, to the amount of strain relaxation and to the SiGe material parameters.

V. SUMMARY AND CONCLUSIONS

We have made Si/SiGe RTD's using nanofabrication techniques. Both cylindrical dots and rectangular wires were fabricated, with lateral dimensions between 230 nm and 10 μm. The low-temperature I-V characteristics showed two resonances, which were due to tunneling via the HH_0 and LH_0 quantum-well subbands. In the dots a strong reduction of $V_p^{\mathrm{LH}_0}$ was observed as the dots became smaller. The HH_0 peak voltage, on the other hand, was independent of dot diameter. In the wires, on the contrary, the peak voltages showed no dependence on the wire width, an unexpected effect. These results arise from the effect of uniaxial and biaxial strain relaxation on the HH-LH splitting and on the HH and LH barrier heights. The in-plane anisotropy of the LH_0 subband was determined with angle-resolved magneto-tunneling spectroscopy. In the dots and in the widest wire the subband was approximately fourfold rotational symmetric. For decreasing wire width the anisotropy gradually changed and had a twofold rotational symmetry. This result can also be explained by partial uniaxial strain relaxation.

In conclusion, we have successfully used Si/SiGe RTD's to study the effect of strain relaxation on the hole subbands in a quantum well. In particular, two strain-dependent properties of the subbands were studied: the subband energies and (the anisotropy of) the in-plane dispersion. The device geometry determines the type of strain relaxation. Biaxial relaxation in dots leads to a severe lowering of the LH_0 subband-edge energy, whereas uniaxial relaxation in wires leaves the subband-energies largely unchanged. Further, we have presented evidence that uniaxial strain relaxation modifies the in-plane dispersion of the LH_0 subband strongly.

ACKNOWLEDGMENTS

We wish to thank B. de Lange for molecular-beam epitaxy growth of the samples, F. D. Tichelaar at the National Center for High Resolution Electron Microscopy for TEM analysis, and J. E. Dijkstra and W. Th. Wenckebach for valuable discussions and for help on the analysis of the strain dependence of the valence band. We acknowledge G. E. W. Bauer for critical reading of the manuscript. This work is part of the research program of the Stichting voor Fundamenteel Onderzoek der Materie (FOM), which is financially supported by the Nederlandse Organisatie voor Wetenschappelijk Onderzoek (NWO).

[1] S. C. Jain, H. E. Maes, K. Pinardi, and I. de Wolf, J. Appl. Phys. **79**, 8145 (1996), and references therein.

[2] J. P. A. van der Wagt, A. C. Seabaugh, and E. Beam III, *IEDM Technical Digest 1996* (IEEE, New York, 1996), pp. 425–428.

[3] A. Zaslavsky, K. R. Milkove, Y. H. Lee, B. Ferland, and T. O. Sedgwick, Appl. Phys. Lett. **67**, 3921 (1995).

[4] R. K. Hayden, D. K. Maude, L. Eaves, E. C. Valadares, M. Henini, F. W. Sheard, O. H. Hughes, J. C. Portal, and L. Cury, Phys. Rev. Lett. **66**, 1749 (1991).

[5] U. Gennser, V. P. Kesan, D. A. Syphers, T. P. Smith III, S. S. Iyer, and E. S. Yang, Phys. Rev. Lett. **67**, 3828 (1991).

[6] A. Zaslavsky, T. P. Smith III, D. A. Grützmacher, S. Y. Lin, T. O. Sedgwick, and D. A. Syphers, Phys. Rev. B **48**, 15 112 (1993).

[7] S. Y. Lin, A. Zaslavsky, K. Hirakawa, D. C. Tsui, and J. F. Klem, Appl. Phys. Lett. **60**, 601 (1992).

[8] R. K. Hayden, E. C. Valadares, M. Henini, L. Eaves, D. K. Maude, and J. C. Portal, Phys. Rev. B **46**, 15 586 (1992).

[9] B. Dietrich, E. Bugiel, H. J. Osten, and P. Zaumseil, J. Appl. Phys. **74**, 7223 (1993).

[10] S. C. Jain, B. Dietrich, H. Richter, A. Atkinson, and A. H. Harker, Phys. Rev. B **52**, 6247 (1995).

[11] A. Zaslavsky, D. A. Grützmacher, S. Y. Lin, T. P. Smith III, R. A. Kiehl, and T. O. Sedgwick, Phys. Rev. B **47**, 16 036 (1993).

[12] H. C. Liu, D. Landheer, M. Buchanan, D. C. Houghton, M. D'Iorio, and Song Kechang, Superlattices Microstruct. **5**, 213 (1989).

[13] C. D. Akyüz, A. Zaslavsky, L. B. Freund, D. A. Syphers, and T. O. Sedgwick (unpublished).

[14] M. W. Dellow, P. H. Beton, C. J. G. M. Langerak, T. J. Foster, P. C. Main, L. Eaves, M. Henini, S. P. Beaumont, and C. D. W. Wilkinson, Phys. Rev. Lett. **68**, 1754 (1992).

[15] W. Zawadzki, Semicond. Sci. Technol. **2**, 550 (1987).

[16] C. G. van de Walle, Phys. Rev. B **39**, 1871 (1989).

[17] *Numerical Data and Functional Relationships in Science and Technology*, edited by O. Madelung, Landolt-Bornstein, New Series Group III, Vol. 17, Pt. a (Springer, Berlin, 1982); the Si value of a_v was taken from J. D. Wiley, in *Transport Phenomena*, edited by R. K. Willardson and A. C. Beer,

Semiconductors and Semimetals Vol. 10 (Academic, New York, 1975).
[18] C. G. van de Walle and R. M. Martin, Phys. Rev. B **34**, 5621 (1986).
[19] J. M. Hinckley and J. Singh, Phys. Rev. B **42**, 3546 (1990).
[20] T. Manku and A. Nathan, J. Appl. Phys. **73**, 1205 (1993).
[21] R. Wessel and M. Altarelli, Phys. Rev. B **40**, 12 457 (1989).
[22] G. Dresselhaus, A. F. Kip, and C. Kittel, Phys. Rev. **98**, 368 (1955).
[23] G. Schuberth, G. Abstreiter, E. Gornik, F. Schäffler, and J. F. Luy, Phys. Rev. B **43**, 2280 (1991).
[24] F. F. Fang and W. E. Howard, Phys. Rev. Lett. **16**, 797 (1966).